*Laser and Particle Beams* (2001), *19*, 509–525. Printed in the USA.

DOI: 10.1017.S0263034601194012

# *Z* pinches—A historical view

R.B. SPIELMAN[1] AND J.S. DE GROOT[2]

[1]Sandia National Laboratories, Albuquerque, NM 87185-1194, USA
[2]Department of Applied Science and Plasma Research Group, University of California, Davis, Davis, CA 95616, USA

(Received 22 May 2000; Accepted 20 April 2001)

**Abstract**

*Z* pinches have a long and varied history. Beginning in the 18th century, *z* pinches have been used to heat plasmas very efficiently. Early in the nuclear fusion program, it was realized that modest currents are required to confine plasma that could produce energy gain. The instability of the confined plasma was convincingly demonstrated in experiments in the 1950s that were performed around the world. These uniformly negative results led to *z* pinches being dropped as a fusion concept. Recent progress in fast *z* pinches has reinvigorated the field. We review the field and highlight the recent advances that point the way to a bright future for *z* pinches.

## 1. INTRODUCTION

A *z* pinch in its simplest form is a column of plasma through which current is driven in the axial ($z$) direction by an electrical power source, thus producing an azimuthally directed magnetic field that tends to confine the plasma (see Fig. 1).

The history of *z* pinches is also the history of the development of plasma physics. The earliest *z* pinches were driven by electrostatic generators and used to create electrical breakdown in air. Van Marum's very large generator was constructed in 1784 (Turner & Levere, 1973). It could produce a spark 60-cm long (Finn, 1971) which implies a peak voltage of about 0.33 MV. The estimated capacity (Finn, 1971) was 0.56 $\mu$F so it could store up to 30 kJ! This generator is presently located in the Teyler museum in the Netherlands.

*Z* pinches have wide application because they are a very efficient way to heat and/or confine high-temperature plasma that can be used to efficiently generate X rays and/or to possibly produce conditions required for thermonuclear fusion. Modern *z* pinch development and plasma physics began in 1934 when Bennett (1934) showed that the current required to confine a uniform plasma column ($B^2/2\mu_0 = \mathrm{P}$) with radius $r_p$, electron density, $n_e$, and electron and ion temperature, $T$, is:

$$I_c\,(\mathrm{MA}) \approx 1.4 \times 10^{-9} r_p\,(\mathrm{cm}) \sqrt{n_e\,(\mathrm{cm}^{-3}) T\,(\mathrm{keV})}. \qquad (1)$$

Address correspondence and reprint requests to: R.B. Spielman, MS-1194, P.O. Box 5800, Albuquerque, NM 87185-1194, USA. E-mail: rbspiel@sia.gov

Depending on the application, the plasma density and temperature are chosen to reach the required fusion yield and/or X-ray power. The key point is that remarkably low currents are required to confine high-density high-temperature plasma, for example, for $n_e \approx 10^{19}$ cm$^{-3}$, $T_e \approx 5$ keV, $r_p \approx 1$ mm, $I_c \approx 1$ MA. Typically, the minimum column radius and maximum confinement time is limited by magneto-hydrodynamic (MHD; Liberman *et al.*, 1999, Chap. 4) or magneto-Rayleigh–Taylor (MRT; Liberman *et al.*, 1999, Chap. 5) instabilities. (We see why most *z*-pinch research has been aimed at mitigation of plasma instabilities.)

The simple Bennett relationship was further refined independently by Pease (1957), and Braginskii (1957), who assumed energy steady state and equated the resistive heating to Bremsstrahlung cooling by the assumed thin hydrogenic plasma. The result is the classic Pease–Braginskii current.

$$I_{PB}\,(\mathrm{MA}) \approx 0.7\,\frac{Z+1}{Z}\,[\lambda \ln(\Lambda/10)]^{1/2}, \qquad (2)$$

where $Z$ is the average ion charge, $\ln \Lambda$ is the Coulomb logarithm, and the factor $\lambda$ is a numerical factor depending on the temperature, density, and current density profiles in the *z* pinch. This remarkable result that the current required for force and energy equilibrium only depends on the radial profiles of current, density, and temperature is a consequence of the fundamental connection between the bremsstrahlung opacity and the resistivity. Assuming blackbody radiation is the dominant energy loss results in a quite different result, that is,

$$I \sim n^{2/3}/T^4. \qquad (3)$$

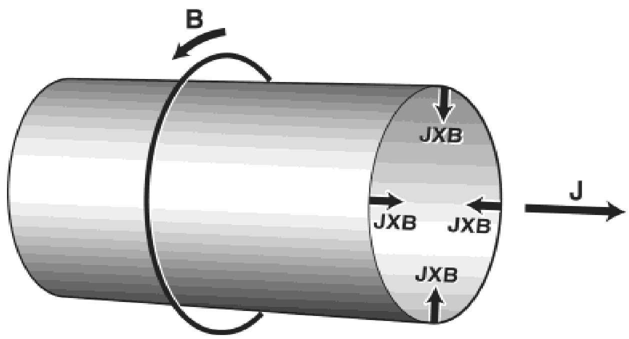


**Fig. 1.** Simple *z* pinch showing an axial current producing a magnetic field that pinches the plasma.

## 2. THE 1950S: *Z* PINCHES FOR FUSION POWER

*Z* pinches, and therefore plasma physics, became an important research area in the 1950s, when scientists at Los Alamos in the United States (summarized in Tuck, 1958), at the Kurchatov Institute in Russia (summarized in Artsimovich, 1958), and in the United Kingdom (summarized in Thronemann, 1958) suggested that D-T *z* pinches could lead to the development of fusion power plants. The initial research program was classified because of strong interlaboratory and international competition and perceived connections to nuclear weapons research. Both linear (Mather & Williams, 1958) and toroidal (Cousins & Ware, 1951; Sakharov, 1951; Tamm, 1951; Thronemann & Gowhig, 1951) geometries were tried. Unfortunately, fast (microsecond time scale) MHD instabilities were observed to disrupt plasma confinement. It was not possible to eliminate the instabilities either experimentally or theoretically, so the respective national laboratories and the fusion community lost interest in *z* pinches as fusion configurations. In recent years there has been a revival of interest in two forms of pinches—the reversed field pinch (RFP; Alper, 1990; Prager, 1992) and the field reversed configuration (FRC; Tuszewski, 1988).

The problem of MHD stability of a quasi-static linear pinch is one of the most intensely investigated subjects in plasma physics. To a large extent, MHD and stability theory was developed in the 1950s, during the early stage of thermonuclear fusion research. The basic stability criteria for MHD systems were established (Kruskal & Schwarzschild, 1954; Rosenbluth *et al.*, 1954; Rosenbluth, 1956; Shafranov, 1956, 1958*a*, 1958*b*; Rosenbluth & Longmire, 1957; Suydam, 1958). Then the Energy Principle was formulated (Rosenbluth & Longmire, 1957; Bernstein *et al.*, 1958; Furth, 1963; Grad, 1966) as a way of quantifying the plasma instabilities. Finally, the equations describing the MHD approximation of the eigenmodes of a *z* pinch (including the unstable ones) were derived (Tayler, 1957; Hain *et al.*, 1957; Kruskal & Oberman, 1958; Chandrasekar, 1961) and their solutions were found for some simple *z*-pinch configurations (Shafranov, 1956, 1958*a*; Tayler, 1957; Trubnikov, 1958; Furth, 1963; Coppi, 1964*a*, 1964*b*, 1965; Coppi *et al.*, 1966). The stability criteria were deduced from the Energy Principle, and three important stability conditions were obtained: the Kruskal–Shafranov limit, the Suydam criteria, and the Newcomb theorem. The results of this research were not optimistic for a *z* pinch regarded as a magnetic confinement fusion system. Theory demonstrated poor stability of a steady-state simple *z* pinch, which in almost any case exhibited hydromagnetic instabilities with growth rates on the order of the inverse Alfvén transit time. These theoretical conclusions were confirmed by many experiments (Anderson *et al.*, 1958; Gorbunov & Rosumova, 1963; Artsimovich *et al.*, 1964).

The physics of magnetized plasmas developed in this exciting period laid the foundations for all modern plasma physics. This is demonstrated today by the continued research in magnetically confined plasma geometries such as the Tokamak and the Stellerator, to name just two.

## 3. THE 1960S: *Z* PINCHES AS X-RAY SOURCES

The fast escape of confined plasma led to the virtual elimination of quasi-static *z*-pinch concepts from the worldwide thermonuclear fusion research program. The thermonuclear fusion research program went down a different path. More complicated magnetic field configurations (field-reversed configurations, etc.) and/or low $\beta$ ($\beta = 2\mu_0 P/B^2$, where $P$ is the plasma pressure and $B$ is the magnetic field) toroidal configurations (TOKAMAK, etc.) were used in an attempt to reduce or eliminate the MHD instabilities. The next development in *z*-pinch research was the realization in the 1960s that *z* pinches could be used as efficient UV, XUV, and soft X-ray generators. These intense *z*-pinch X-ray sources were to play a major role in the field of nuclear weapon effects and material hardening over the next 30+ years.

The first *z*-pinch soft X-ray sources were exploding wires (Chace & Moore, 1959–1968). Typically a voltage of 10s of kilovolts from a charged capacitor was applied to a fine wire of about 10–100 $\mu$m in diameter in time scales of $\sim$1 $\mu$s. At first, the wire material is heated. Then the wire surface vaporizes and the current decreases. As the electric field increases and the vapor expands, breakdown takes place. A low-resistance, low-density plasma is created in which most of the current flows, and the plasma pinches nonuniformly along the wire. With both ohmic and compressional heating, the plasma reaches temperatures of 10–100 eV and radiates a blackbody spectrum since the absorption mean free path is much less than the diameter of the plasma. The plasma electron density after pinching is typically about $10^{21}$ cm$^{-3}$. Depending on the instabilities formed during the wire explosion and the particular wire material, the radiation spectrum can be strongly nonthermal. *L*-shell and *K*-shell radiation having photon energies far greater than the thermal Planckian spectrum can be radiated from localized regions.

https://doi.org/10.1017/S0263034601194012 Published online by Cambridge University Press

J. C. Martin led the development of nanosecond pulsed-power technologies that have had a huge impact in the field of *z* pinches (Martin *et al.*, 1996). Developments in pulsed power engineering and physics came rapidly and culminated with the development of MV-, MA-, and TW-class drivers: Gamble I and II located at the Naval Research Laboratories in Washington D.C., Blackjack 3 at Maxwell Laboratories in San Diego, California, and Pithon at Physics International Company in San Leandro California, and one module of Angara 5 at the Kurchatov Institute, USSR. These machines relied on Marx generators, water capacitors, and magnetically insulated transmission lines. These new, fast accelerators were used to drive single wires with fascinating results. Very intense X rays were observed from exploding single wires of various atomic compositions at the Naval Research Laboratory in 1969 (Shanny & Vitkovitsky, 1969; Mosher *et al.*, 1973). Previous experiments had involved electrical powers of $<$100s GW; this new pulsed-power technology made possible electrical powers of $\sim$1 to 2 TW. As a result, it was possible to reach plasma temperatures where the plasma (about 1-mm diameter and densities in the range $\sim 10^{21}$ cm$^{-3}$) became optically thin and the temperature was therefore not limited by the radiation law of a blackbody. The resulting radiation powers were on the order of the power of the pulsed-power drivers.

The high initial impedance of single exploding wires, typically 1–2 Ω, limits scaling to higher X-ray powers. Scaling these systems to higher currents to reach higher X-ray energies and powers would have required pulsed-power systems of very high power ($>$100 TW), resulting in extremely high voltages ($\gg$10 MV). This pulsed-power engineering limitation led to the reexamination and further development of dynamic *z* pinches as X-ray sources (Linhart *et al.*, 1962; Turchi & Baker, 1973; Stallings *et al.*, 1979; Katzenstein, 1981) A simple argument demonstrates the advantage of using a pulsed-power system to implode a plasma as compared to resistive and compressional heating. The pulsed-power system must drive an axial current through a cylindrical *z*-pinch load to stagnation. The stagnation plasma must be dense enough (ion–ion mean free path much smaller than the plasma radius at stagnation) that the implosion energy is converted to electron thermal energy and radiated. Also, the final heating rate must be high enough to overcome the initial radiation losses in order to reach the desired plasma temperatures. The initial inductance (impedance) of the *z* pinch is low due to its relatively large diameter. The voltage applied to the load is well approximated by

$$V = L(dI/dt) \sim LI_{max}/\tau, \tag{4}$$

where $L$ is the inductance, $I_{max}$ is the maximum current, and $\tau$ is the rise time of the current pulse. With electrical time scales on the order of 100 ns and inductances on the order of 10 nH, the voltages required to reach the MA level are well within the capabilities of modern pulsed-power systems. The radial velocity of the load at stagnation is

$$v \propto I_{max}/M_L^{1/2}, \tag{5}$$

where $M_L$ is the linear mass of the load. The radial implosion energy of the ions is rapidly converted to electron temperature,

$$T_e \sim v^2 \sim \tau^2 V^2/(L^2 M_L), \tag{6}$$

on the time scale of the stagnation of the mass on axis. Higher electron temperatures can be reached by coupling more energy at higher implosion velocities as compared to resistive and compressional heating where higher voltages are required to reach temperatures above a few hundred electron volts.

## 4. A REBIRTH OF *Z* PINCHES IN THE 1970S

Theoretical predictions that fast *z* pinches would be more stable to MRT instabilities led to growth in *z*-pinch research for X-ray sources. A simple argument demonstrates why faster implosions are more stable. The total number of e-folding that the classical MRT instability (with growth rate $(ka)^{1/2}$, where $k$ is the wave number of the growing perturbation and $a$ is the acceleration) grows during the time that the load is accelerated (for constant acceleration) up to velocity, $v$, is proportional to $v/a^{1/2}$. We see that increasing the acceleration over a shorter period of time, that is, faster implosions are more stable if a given implosion velocity is required.

This realization of improved plasma stability coupled with the rapid development of pulsed-power technology led to numerous suggestions for the use of *z* pinches. Some of these ideas were improvements on earlier fusion schemes. An important idea was the use of fast *z* pinches for inertial confinement fusion. This was pursued hotly by researchers at Physics International (Stallings *et al.*, 1979), Sandia National Laboratories (Freeman *et al.*, 1977; Clauser *et al.*, 1978; McDaniel *et al.*, 1979*a*, 1979*b*), and Kurchatov Institute for Atomic Energy (Rudakov, 1979*a*, 1979*b*).

While these ideas for inertial confinement fusion were sound, many were ahead of their time, needing to await the development of improved computational capabilities, better plasma diagnostics, and larger pulsed-power drivers.

One of the first dynamic load configurations proposed was the annular liner (Linhart, 1962). Experiments conducted at the Air Force Weapons Laboratory on the Shiva–Star facility (1975–1980) demonstrated the utility of aluminum liners for microsecond time-scale *z*-pinch experiments (Turchi & Baker, 1973; Burns *et al.*, 1977; Baker *et al.*, 1978). These first long-pulse experiments clearly demonstrated the impact of MRT instabilities. Analytic calculations and computer simulations laid the foundations for understanding the Rayleigh–Taylor instabilities.

The MRT instability was very severe for the long pulses on the Shiva–Star facility. The short pulses available on Proto-II (5 MA, 50 ns) at Sandia National Laboratories provided an alternate test bed to study liner implosions that should have reduced MRT instabilities (McDaniel *et al.*, 1979*a*, 1979*b*; Stinnett *et al.*, 1979).

## 5. THE 1980S: THE BEGINNING OF MODERN PULSED POWER

The 1980s saw the development of the first multimodule electrical drivers for *z* pinches. Electrical power levels now reached 20 TW. The low initial impedance of liner, gas puff, and wire array loads coupled well with the low-impedance, high-current, multimodule electrical drivers being developed at this time. These drivers included: Blackjack 5 (4.6 MA and 10 TW) at Maxwell Laboratories, Inc. in San Diego, California; Double Eagle (3 MA and 8 TW) at Physics International Co. in San Leandro, California; Saturn (11.5 MA and 25 TW) at Sandia National Laboratories in Albuquerque, New Mexico; Angara 5 (4.5 MA and 6 TW) at the Kurchatov Institute of Atomic Energy in Moscow and Troitsk; and GIT- 4 (1 MA) and GIT- 8 (4 MA) at the Institute of High Current Electronics in Tomsk, Russia.

Progress was made very quickly during this period. Numerous variations of liner, wire array, and gas-puff loads were developed and tested at many laboratories. These produced prodigious amounts of data that enabled rapid progress in understanding *z* pinches. At the same time, the ability to model *z* pinches was greatly improved. Experiments with gas-puff *z* pinches and wire-array *z* pinches conclusively demonstrated that modern, fast *z*-pinch systems were capable of greater stability and provided higher compression, much greater energy density, and longer plasma confinement times than predicted by the conventional estimates from the 1950s and 1960s. Pereira and Davis (1988) gave a comprehensive review article on *z*-pinch research. *Z* pinches were now generating X-ray powers at levels previously attainable only on very costly lasers like the NOVA laser (Campbell *et al*., 1986) at the Lawrence Livermore National Laboratory in Livermore, California.

### 5.1. Cylindrical liners

Liner experiments on Proto-II (5 MA, 50 ns) and, later, on Saturn (10 MA, 50 ns; Hsing *et al*., 1990; McDaniel *et al.*, 1992) at Sandia National Laboratories (SNL) confirmed the utility of aluminum liners for *z*-pinch X-ray sources. These experiments also showed that the development of the MRT instability was enhanced by poor liner quality. This was exaggerated by the low masses required on Proto-II. The aluminum early liners fabricated for Saturn had thicknesses of ~200–300 nm and had large azimuthal and axial wrinkles (see Fig. 2). Later aluminum liners fabricated by Los Alamos National Laboratory were greatly improved and, while very fragile, had nearly optically perfect surface finishes (see Fig. 3). Even with excellent liner quality, MRT instabilities developed rapidly. Data using aluminum liners on Saturn gave total X-ray pulse widths just under 20 ns. X-ray pinhole camera data confirmed that the final pinch had strong axial nonuniformities that were consistent with MRT instabilities.

### 5.2 Gas-puff *z* pinches

The 1980s also saw the maturation of the dynamic *z* pinch in the area of gas-puff loads. These gas-puff *z* pinches represented an important class of dynamic *z*-pinch devices (Shiloh *et al*., 1978; Burkhalter *et al*., 1979; Stallings *et al*., 1979; Baksht *et al*., 1981; Marrs *et al*., 1983; Matzen *et al*., 1986; Dukart *et al*., 1987; Felber *et al*., 1988*a*, 1988*b*). The imploding annular gas sheet is a supersonic jet emitted by a gas-injection nozzle in the cathode, directed to the anode; the gas is ionized by the main current pulse or preionized before it. To avoid initial nonuniformities in the gas flow, the anode is a honeycombed transparent structure, so that the gas jet propagates through the anode plane without reflection (Wessel *et al*., 1986). This is a very convenient way to obtain a relatively dense plasma sheet of macroscopic thickness and adjustable line mass. Typical number densities of the neutral gas in the gas puff are $n_0 \sim 10^{17}$–$10^{18}$ cm$^{-3}$. Note the application of gas-puff *z* pinches to very high current devices can be limited because of the required high initial mass. Depending on the atomic *Z* of the desired gas, this requirement leads to very high gas densities that may not be readily available from gas-puff sources. Large compressions have been obtained with large-diameter gas-puff loads (~30-fold compression, Spielman *et al*., 1995). Kinetic effects are suggested to reduce the MRT growth rate in these low-density gas-puff loads (De Groot *et al.*, 1997*b*). Gas-puff *z* pinches have been used as a flashlamp for photo-pumping an X-ray laser (Maxon *et al*., 1985; Spielman *et al.*, 1985*a*).

### 5.3. Wire arrays

Wire arrays are attractive *z*-pinch loads because of the low fabrication cost and the high quality (axial and radial uniformity) that can be obtained. This is especially true for smaller, low-current drivers where the mass needed for the load makes the fabrication of liners very difficult. The limitation in wire array loads is the availability of small diameter wire. Thus we see that smaller machines typically used fewer wires than larger machines and that much of the early data on wire arrays was dominated by low wire number experiments. The ease of fielding wire array loads led to a large body of data covering different wire materials (Alvazov *et al*., 1988, 1990; Baksht *et al*., 1989, 1993; Bekhtev

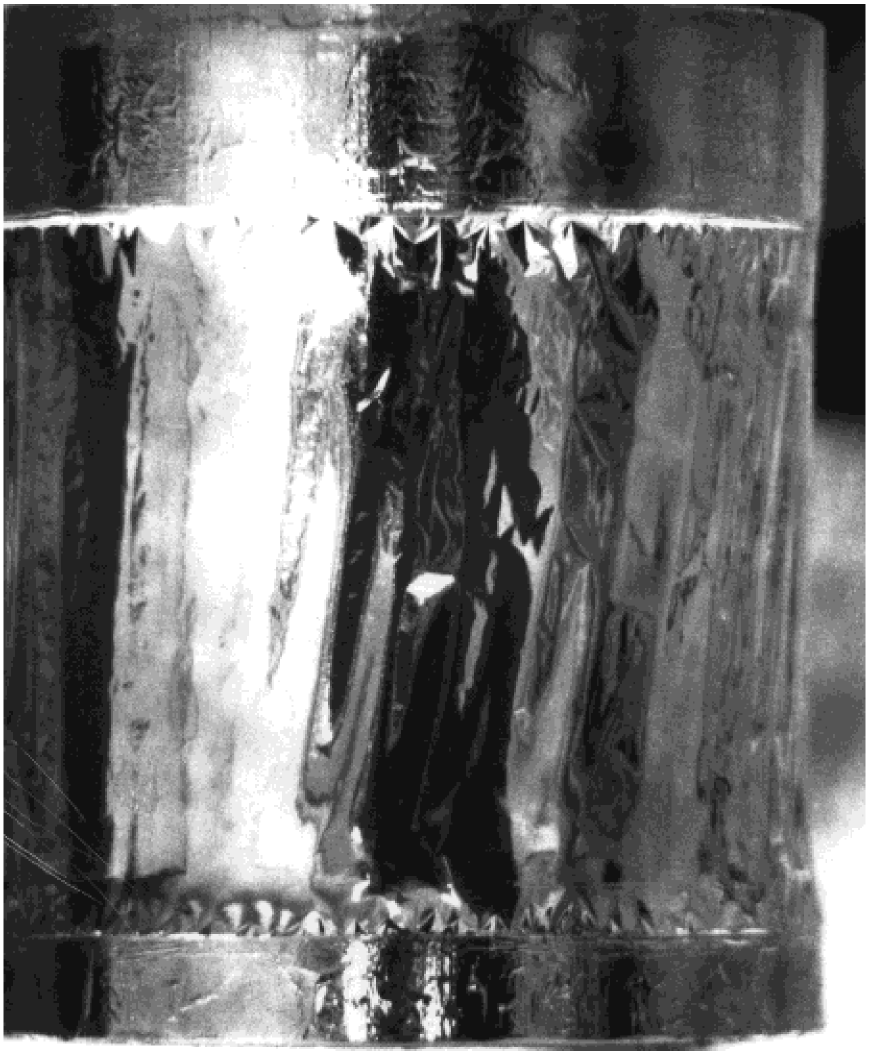

**Fig. 2.** Photograph of a wrinkled liner (1.8-cm diameter and 2-cm length; McDaniel *et al.*, 1992).

*et al.*, 1989; Deeney *et al.*, 1989, 1991, 1994; Spielman *et al.*, 1989, 1994; Vikharev *et al.*, 1991; Whitney *et al.*, 1994). Experiments indicated (Spielman *et al.*, 1994) that the pinch reaches a minimum diameter of as small as 1 mm (depending on the load parameters) and remains at approximately this diameter for many Alfvén transit times, indicating that the pinch is in force equilibrium. The pinch develops a complex, apparently helical, structure during an expansion phase after stagnation. The more uniform the final pinch (the smaller the final pinch diameter), the smaller the diameter of the helix that is formed. Spielman *et al.* (1994) emphasized that the integrated and apparent brightness of the images increases during the equilibrium phase, so that energy is dissipated in the pinch. Large-scale-length MHD instabilities are evident at 15 ns (Spielman *et al.*, 1994), and X-ray emission greatly increases. The excellent (approximately nanosecond) agreement between observed, experimental, and calculated implosion times indicates that the vast majority of the initial mass of the wire array is imploded and reaches stagnation.

## 6. THE 1990S: THE WIRE ARRAY *Z* PINCH AND MJ-CLASS PULSED-POWER DRIVERS

At present it is possible to produce current pulses with peak values as large as 20 MA and rise times on the order of 100 ns, the impedance of modern high-current pulsed-power systems being on the order of 0.1 to 0.25 Ω. The rate of current increase can be as high as $3 \times 10^{14}$ A/s, and the energy delivered to the *z* pinch can be optimized by choosing the initial *z*-pinch geometry, mass, and improving plasma uniformity. The world's largest pulsed-power driver is the Z pulsed-power driver at SNL. A schematic diagram showing the Marx generators, the water pulse-forming sections, the magnetically insulated transmission lines, and a diagnostic line of sight is presented in Figure 4. Z is the latest in a sequence of *z*-pinch drivers at Sandia National Laboratories based on water-dielectric pulse-forming technology. Z stores 11.4 MJ in its 36 Marx generators and couples 5 MJ and 60 TW in a 105-ns full-width-at-half-maximum (FWHM) pulse into 36 constant-impedance 4.32-Ω water transmis-

https://doi.org/10.1017/S0263034601194012 Published online by Cambridge University Press

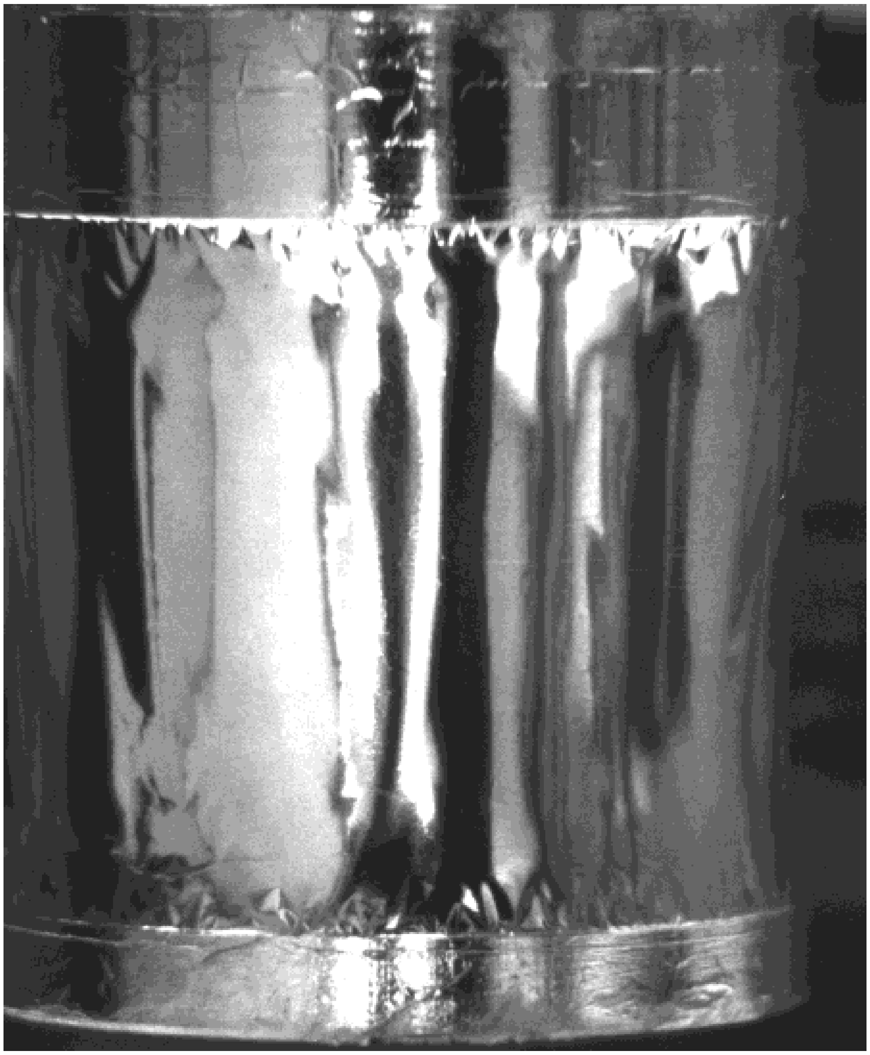

**Fig. 3.** Photograph of a smooth liner (1.8-cm diameter and 2-cm length; McDaniel *et al.*, 1992).

sion lines. In its normal operating mode, Z delivers up to 3.0 MJ and 50 TW of electrical energy to four, separate vacuum insulator stacks. Total currents up to 20 MA are measured at the insulator stack. Current is fed via four magnetically insulated vacuum transmission lines (MITLs) (see Fig. 5) and a vacuum convolute (see Fig. 6) to the *z*-pinch load (see Fig. 7). Depending on the load geometry, power flow configuration, initial inductance (typically 10–12 nH), and the implosion time, ~100–150 ns, peak load currents of 16–20 MA are reached with a time-to-peak current of 105 ns. The constant, 120-mΩ impedance of the long water transmission lines allows us to accurately model the electrical circuit and load coupling with lumped circuit codes.

### 6.1. Wire arrays with large numbers of wires

The observation by Sanford *et al.* (1996) and Deeney *et al.* (1997*a*, 1997*b*) that the X-ray power radiated from a wire array *z* pinch increased rapidly as the number of wires was increased changed the entire *z*-pinch field. In just a few months it became clear that the *z* pinch was capable of X-ray power levels up to four times the electrical power in the accelerator. Saturn, producing 20 TW of X rays for >5 years suddenly was generating >80 TW of X rays. Figure 8 shows a photograph of a modern wire array load used on the Z pulsed-power driver.

The reason for the improvement in performance with increasing wire number seemed intuitively obvious, at least at first glance. A large number of wires (at constant mass) positioned very precisely created an initially more uniform plasma shell. This reduction in the magnitude of the azimuthal density perturbations should have a major effect on the development of the MRT instability. This improved plasma shell should stagnate more quickly and generate higher plasma temperatures and higher X-ray powers. Data show that this is the case. The pinch diameter, temperature, uniformity are all improved with a larger numbers of wires in the wire array. The quantitative details of the relationship between wire number, wire material, and X-ray performance was not so obvious. It rapidly became clear that

https://doi.org/10.1017/S0263034601194012 Published online by Cambridge University Press

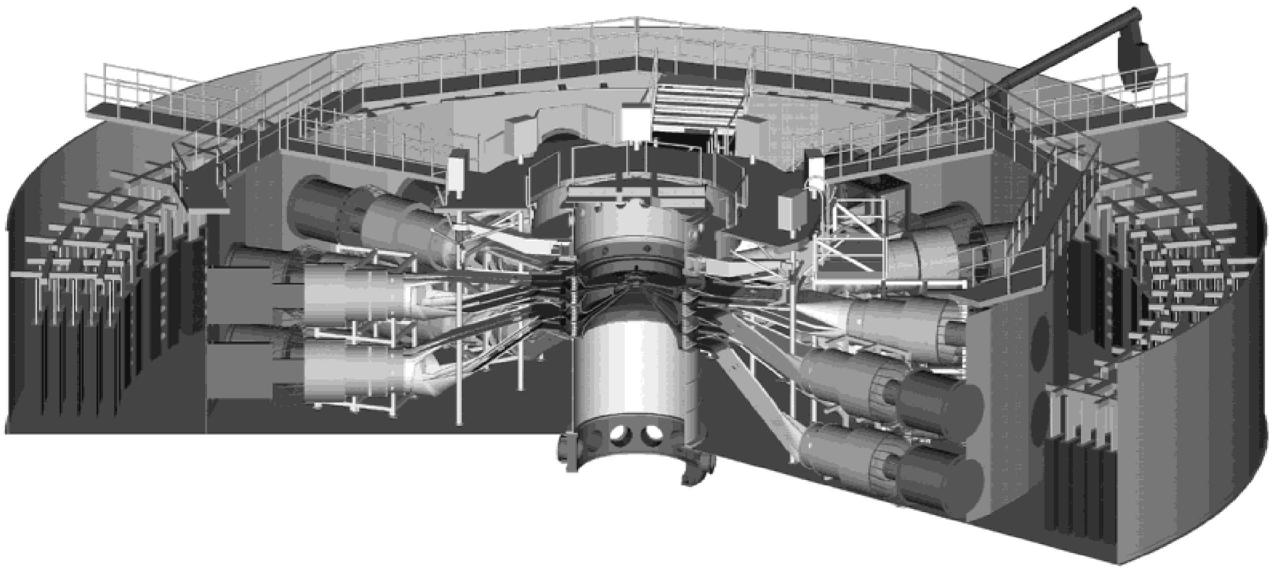

**Fig. 4.** Schematic drawing of the Z pulsed-power driver showing the Marx generators, the water pulse-forming section, and the four MITLs.

wires, especially high-*Z* wires such as tungsten, retained discrete wire characteristics long into the implosion of the *z* pinch. Too few wires may result in wire–wire perturbation effects (Felber & Rostoker, 1981; Hammer & Ryutov, 1999). Too many wires will eventually result in shell-like behavior with its purely MRT behavior. A detailed understanding of the relationship of wire number and pinch quality awaits further data and improved computational capability.

These high-wire number results from the Saturn accelerator greatly accelerated the development of high power X-ray sources proposed for the new Z accelerator. Indeed, the 50-TW Z driver was soon able to generate X-ray powers up to ~200 TW with tungsten wire arrays containing 240 7.5-$\mu$m diameter wires. The scaling of *z*-pinch X-ray power continued to increase with driver power! This significant observation gives us confi-

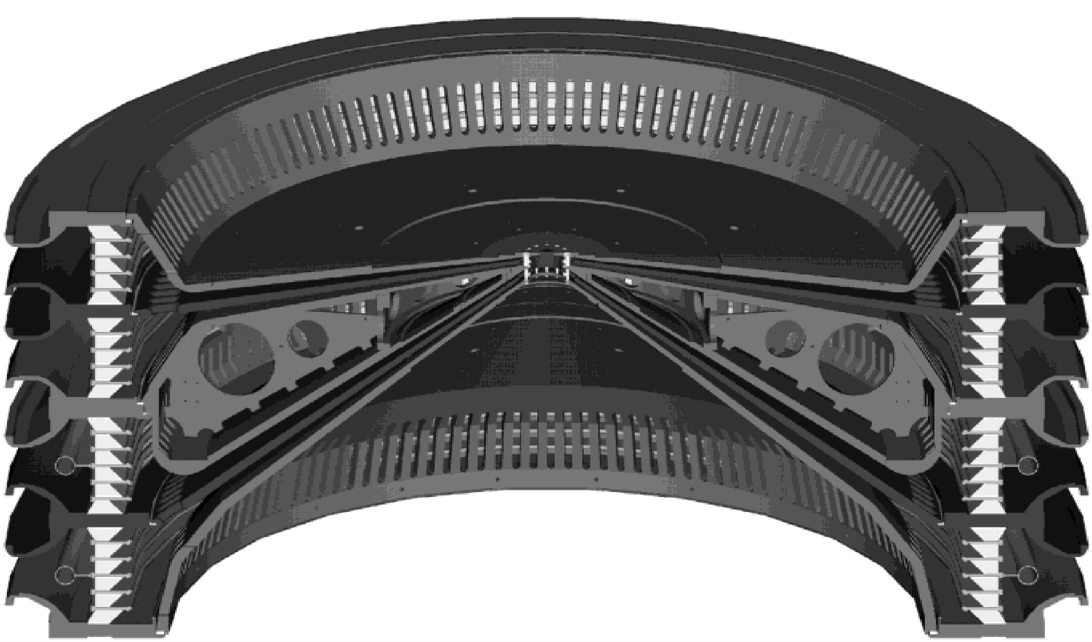

**Fig. 5.** Schematic drawing of the four MITLs that are joined in parallel by a 12-post double-posthole convolute on Z.

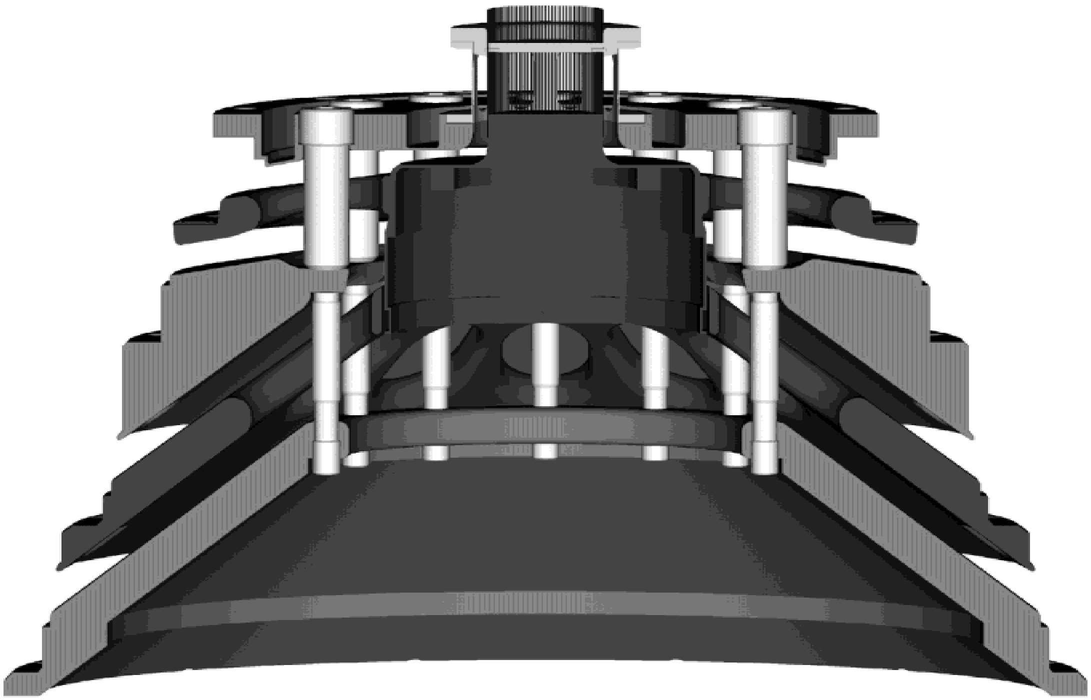

**Fig. 6.** Schematic drawing of the 5-cm-long MITL that connects the convolute to the load.

dence that larger drivers yet can generate higher X-ray powers.

## 6.2. Complex loads and MRT

One always hopes that there is a load configuration that mitigates the impact of instabilities. This is not a new dream, in fact, it is a direct descendent of the thinking surrounding quasi-static linear pinches in the 1950s. It always seemed that the proper application of some parameter such as magnetic fields or mass accretion would stabilize these MHD instabilities. We now know that it is impossible to completely stabilize a dynamic *z* pinch. Parameters, such as acceleration, that drive the growth of instabilities *must* exist

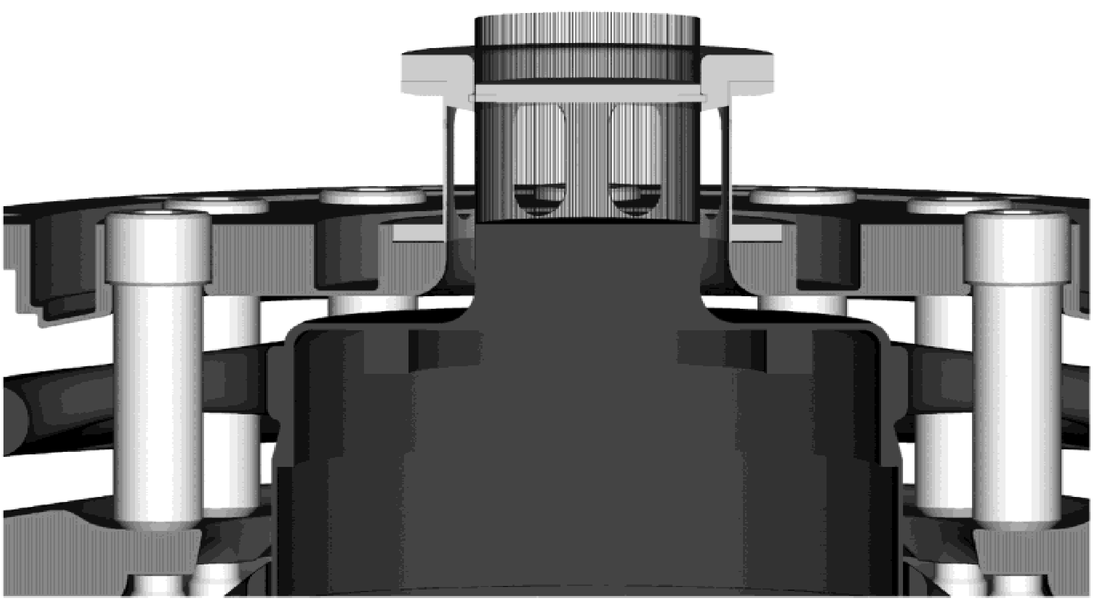

**Fig. 7.** Schematic drawing of the posthole convolute and a typical wire array load on Z. A typical wire array load is 1–2 cm tall with a 3–5-mm radial anode gap.

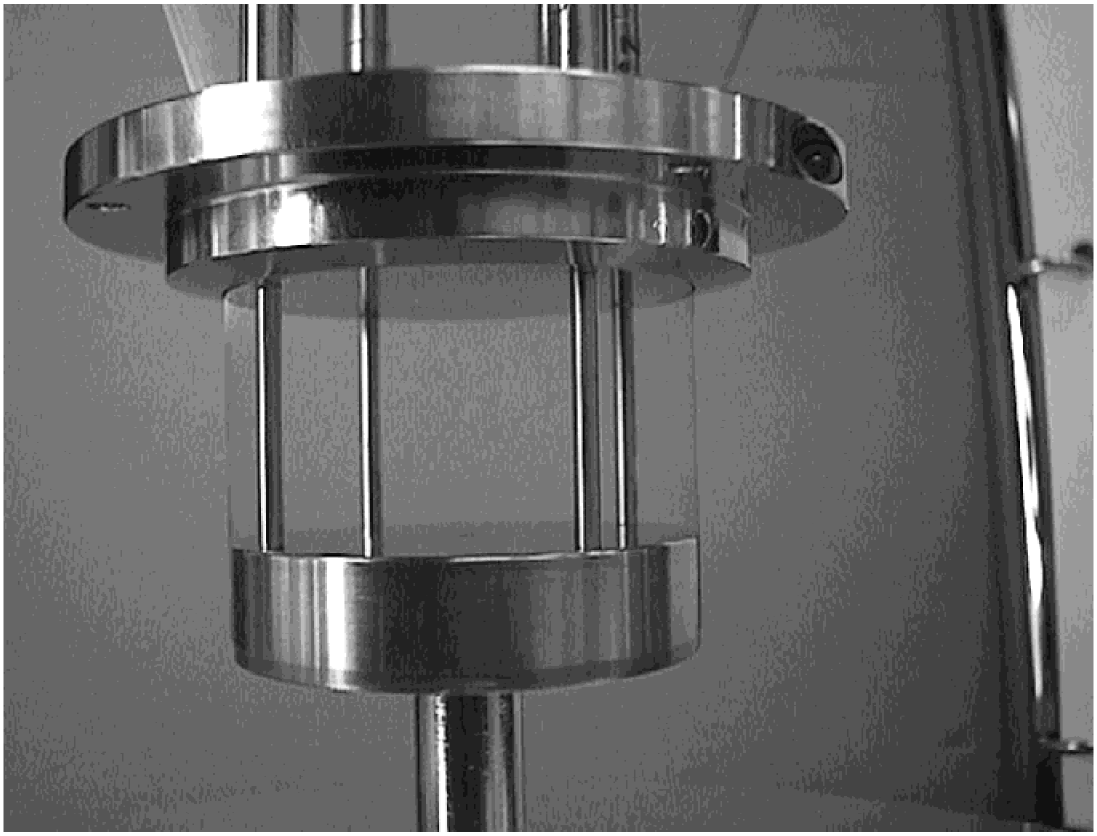

**Fig. 8.** Photograph of a wire array load used on Z (shot 373). The array diameter (length) is 4 cm (2 cm) with 480 7.5-$\mu$m-diameter tungsten wires.

or there is effectively no *z* pinch. The Second Law of Thermodynamics demands that any factor that acts to stabilize an MHD instability must be paid for with energy. In most cases this is seen as dissipation. The greater the level of stabilization, the greater the level of dissipation. However, in many cases for *z*-pinch radiation sources even a minor mitigation of MRT might have dramatic benefits in radiation power or peak pinch density.

The total growth of the MRT instability during the implosion can be reduced by accreting mass to the shell both during the linear phase (Velikovich & Gol'berg, 1993; Gol'berg & Velikovich, 1994; Hammer *et al*., 1996; Velikovich *et al*., 1996; De Groot *et al*., 1997*a*) and the nonlinear phase (Book, 1996) of the implosion. There are several possible configurations that can accomplish this feat. The acceleration of the sheath driving the MRT instability can be reduced by making a continuous density profile of a certain shape (Hammer *et al*., 1996; Velikovich *et al*., 1997) or the uniform density profile can be replaced by one or more discrete shells. Additionally, axial magnetic fields or other techniques can be used to reach the same result.

Nested shells have been suggested to reduce the effect of the MRT instability. This technique has been tried experimentally (Baksht *et al*., 1994, 1995; Sorokin & Chaikovsky, 1994) using multiple gas-puff shells. Nested-wire arrays (Deeney *et al*., 1998) on the 20-MA Z accelerator at SNL have produced X-ray powers up to 280 TW, have reduced the total X-ray pulsewidth from 5.8 to 4 ns, and have produced pinched plasmas with diameters of only 1 mm with good axial uniformity. A photograph of a double wire array used on Z is shown in Figure 9.

### 6.3. Longer implosion times and the MRT instability

Next generation drivers with currents above 20 MA will either require higher voltages or longer implosion times. Higher voltage results in higher driver cost and higher power-flow risk. Another approach is to lengthen the implosion time and therefore shift the risk to the *z*-pinch load configuration, since simple arguments suggest that the FWHM of the X-ray pulse will be increased, resulting in decreased peak X-ray power. This approach is being investigated in a series of experimental campaigns on Saturn (Deeney *et al*., 1999) and Z (Spielman *et al*., 1998) drivers. Deeney *et al*. (1999) used high wire number, 25-mm-diameter tungsten wire arrays on the 8-MA Saturn driver operating in a long-pulse mode. By varying the mass of the arrays from 710 mg/cm to 6140 mg/cm, implosion times of 130–250 ns have been obtained with implosion

https://doi.org/10.1017/S0263034601194012 Published online by Cambridge University Press

**Fig. 9.** Photograph of a double wire array load used on Z (shot 379). The outer (inner) array has a diameter of 4 cm (2 cm) and 480 (240) 7.1- (7.5)-$\mu$m diameter tungsten wires.

velocities of 50–25 cm/$\mu$s, respectively. These *z*-pinch implosions produced plasmas with millimeter diameters that radiated 600–800 kJ of X rays, with powers of 20–49 TW; the corresponding pulsewidths were 19–7.5 ns, with rise times ranging from 6.5 ns to 4.0 ns. These powers and pulsewidths are similar to those achieved with 50-ns implosion times on Saturn. Two-dimensional, radiation-MHD (RMHD) calculations indicate that the imploding shells in these long implosion time experiments are comparable in width to those in the short-pulse cases. Deeney *et al*. (1999) suggested that this could be due to lower initial perturbations. A heuristic wire array model suggests that the reduced perturbations, in the long-pulse cases, may be due to the individual wire merger occurring well before the acceleration of the shell. The experiments and modeling suggest that 150–200 ns implosion time *z*-pinches could be employed for high-power, X-ray source applications.

### 6.4. MHD simulation of *z* pinches

Computers and RMHD codes had matured by the 1990s to the point that 2-D RMHD simulation codes could be used to calculate the performance of dynamic *z* pinches. To date, extensive calculations have been performed with 2-D (mainly *r*–*z*) RMHD codes. These codes are computationally intensive, because the MHD equations, along with an equation of state, radiation transport, and the distribution of atomic states, must be calculated.

Hammer *et al*. (1996) have used a 2-D (RMHD) Lagrangian code (Zimmerman *et al*., 1973; Nielson & Zimmerman, 1981) to simulate the dynamics of imploding aluminum wire-array and Ne-Ar gas-puff implosions on the Saturn pulsed-power accelerator, and compared these results with measurements. The code uses a multigroup diffusion model to calculate radiation transport with frequency-dependent emissivity and opacity determined by the average atom model (Lokke & Grassberger, 1977; Post *et al*., 1977). Local thermodynamic equilibrium (LTE) is used to calculate the ionization level of the atoms and atomic level populations. The equation of state is based on the Thomas–Fermi–Cowan model (More *et al*., 1975) and the Lee and More (1984) extension of Spitzer resistivity and electron thermal conductivity is included.

Sanford *et al*. (1996, 1997) presented measurements and 2-D RMHD simulations of imploding aluminum wire-array implosions driven by the Saturn accelerator. The simple model of the growth of the classical MRT instability gives the total number of e-foldings as $n_{eff} \sim 15$ for a 1-mm wavelength. Thus the MRT instability is predicted to grow

https://doi.org/10.1017/S0263034601194012 Published online by Cambridge University Press

to large amplitude early in the implosion. The simulations show that the MRT instability grows at short wavelengths (initially $\ll$1 mm, with even larger values of $n_{eff}$), seeds longer wavelengths, and produces the classic bubble-and-spike structure during the implosion. The main X-ray pulse begins when the bubble reaches the axis, resulting in the conversion of the implosion energy to thermal energy, and the electrons in the bubble region are heated to high temperature. The radial smearing of the mass from the breakup into bubble-spikes sets the time scale for the stagnation on axis to $t_{stag} = t_{spike} - t_{bubble}$, where $t_{spike}$, $t_{bubble}$ are the arrival times for the spike tip and bubble, respectively. Since the radiation is produced when kinetic energy is converted to thermal energy, the output-radiation pulse also occurs in a time on the order of $t_{stag}$.

In the simulation, the radiating region contains ~10–20% of the total mass in a region of very small size (~10s of microns), with the bulk of the material at scales on the order of 0.5–1 mm. The FWHM of the radiating region near maximum emission is ~0.05 $\mu$m in the simulations, compared to a measured value of about 0.6 $\mu$m closer to the bulk-plasma radius found in the simulation. The emission tends to be localized near the position on axis where the spike plasma converges. This is in disagreement with the comparatively weak axial structure seen in the experimental images. Radiation cooling plays an important role in the convergence of a fraction of the mass to high density, just as in the more extreme radiative collapse observed in 1-D RMHD simulations, and is sensitive to the atomic physics model used. In particular, the LTE approximation may overestimate the cooling rates and associated collapse behavior.

The small-diameter region of highly compressed plasma may be due to the assumption of azimuthal symmetry implicit in the 2-D calculations. A very small azimuthal nonuniformity would have little effect on the run-in dynamics and MRT development, but could give imploding mass elements angular momentum that would prevent high convergence. The most important sources are the residual azimuthal nonuniformity after the individual wires have merged the perturbations from the return current posts, and the MRT instability in the azimuthal direction. A fluid element with angular momentum, $\delta M r_0 v_\theta$, conserved during the implosion, would have its azimuthal velocity amplified as $v_\theta \sim r_0/r_f$. The fluid element ceases to converge when $v_\theta^2 \approx v_{imp}^2$. Resistive effects may also play a role. The simulations show behavior late in the implosion similar to the saturation model of Roderick and Hussey (1984), where material from the spikes diffuses into the "throat" of a bubble and partially shorts out the accelerating current. The bubble throat develops flow similar to a MHD nozzle. Enhanced resistivity would increase mass transport into the bubbles and may reduce the current density near $r = 0$ that helps drive radiative collapse. The MHD nozzle effect is also involved in the increased coupling to the circuit found in 2-D versus 1-D simulations, since the plasma acceleration and heating associated with the nozzle flow converts magnetic energy to kinetic and thermal energy. The magnitude of the increased coupling is not known accurately, due to significant energy errors in the calculation.

In the course of the simulated stagnation, mass flows axially away from a spike impact point near the axis. The axial flow from one impact point quickly encounters the opposing flow from a neighboring impact point, causing the flow in this interaction region to turn radially outward. The net result is a complex, circulating flow pattern. The stirring continues throughout the rest of the simulation, and acts to convert magnetic energy to thermal energy through PdV heating, producing about half of the long-lived "tail" on the radiation pulse. Of the remainder, 10–15% of the tail emission can be attributed to ohmic heating, with the rest due to decay of the stored electron and ion internal energy. The plasma relaxes to a state in near pressure balance, with a dense core on the order of 0.5-mm diameter and a hot, low-density, weakly emitting halo (the reverse of the situation during the stagnation, where most of the mass was comparatively cool and at larger radius than the emitting region near the axis). Most of the current flows at fairly large radius throughout the stagnation and, subsequent, near equilibrium phase. This is due to the MHD-nozzle shorting effect, mentioned above, during the stagnation and to the current carried in the hot halo in the near equilibrium phase.

In both the primary pulse and the tail emission, thermalized energy is rapidly converted to radiation. This may explain why the simulation is capable of reproducing the observed radiation pulse while inaccurately modeling the spatial density distributions during stagnation. If the code correctly models the sheath acceleration and MRT breakup, then the stagnation time and kinetic energy are determined. At stagnation, most of the kinetic energy will become thermalized through shock and PdV heating. As long as the stagnation density is sufficiently high, the radiative and electron–ion energy exchange rates are on the order of or faster than the stagnation time, and all of the thermalized energy is radiated with very little sensitivity to the details of the density distribution. In contrast, the energy distribution of the X-ray emission will depend on the details of the magnitude and distribution of density and temperature, which may explain some of the approximately factor-of-2 differences between simulated and experimental spectra.

Peterson *et al*. (1996) used an Eulerian 2-D RMHD code to calculate the dynamics of an imploding-liner *z* pinch, driven by the PEGASUS capacitor bank (capacity = 216 $\mu$F, resistance = 0.3 $\Omega$, inductance = 36 nH, current rise time = 2 $\mu$s, and maximum current = 3 MA). Since the liner is initially solid, Peterson *et al*. (1996) used a 1-D MHD computer code to calculate the initial expansion and to obtain initial plasma parameters to use in the 2-D simulations. The MRT instabilities are predicted to grow to large amplitude, $n_{eff} \gg 1$. The fastest growing instabilities are sausage ($m = 0$, $k \neq 0$) modes, so the nonlinear dynamics can be simulated with a 2-D MHD model. The R-T instability is seen to grow to large amplitude early in the implosion. The usual bubble-

https://doi.org/10.1017/S0263034601194012 Published online by Cambridge University Press

and-spike nonlinear structure then develops. Measurements of liner breakup and healing of the liner are shown to agree with the calculations. The initial amplitudes of the unstable modes are unknown, so the initial amplitude is chosen to obtain good agreement between measured and calculated X-ray emission (pulse shape, peak power, and radiated energy). They find that mode coupling of the MRT modes does not play a role in these implosions. One problem with these calculations is that shorter wavelength, faster growing modes are not resolved in these calculations (the shortest wavelength mode that is well resolved [eight cells/wavelength is required] is ~ 0.4 cm, com-

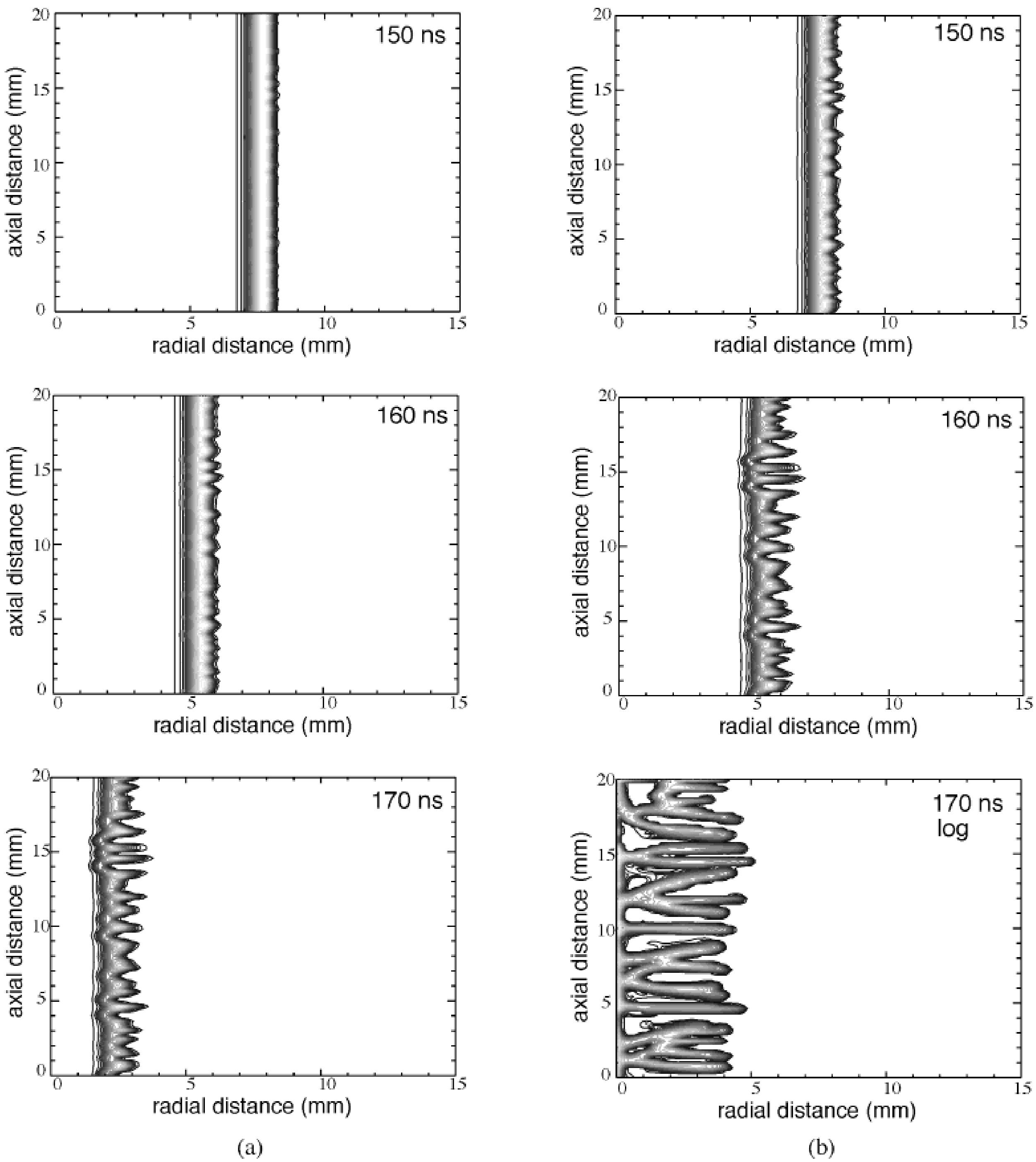


**Fig. 10.** Simulation of a long implosion (Saturn shot 2496) at 150, 160, and 170 ns for (a) an initial 1% cell-to-cell random density perturbation and (b) an initial 20% cell-to-cell random density perturbation. (From Douglas *et al.*, 2000*b*.)

https://doi.org/10.1017/S0263034601194012 Published online by Cambridge University Press

pared to a rough estimate of the fastest growing mode of ~ 0.001–0.01 cm).

Sheehey *et al*. (1992) used a 2-D RMHD code to simulate deuterium-fiber-initiated *Z* pinches. They emphasize that the initial conditions are important in the development of the sausage instability. A low-density corona develops during the initiation process and the sausage instability develops in the corona. The calculations show the rapid development of the sausage instability when the fiber becomes fully ionized. The instabilities drive nonuniform heating and rapid expansion of the plasma column.

Maxon *et al*. (1996) used a 2-D Lagrangian RMHD code (Zimmerman *et al*., 1973; Nielson & Zimmerman, 1981) to study the dynamics of small-initial-diameter (0.4 cm) aluminum wire arrays driven by the Saturn accelerator. The calculations show that the MRT instability dominates the pinch dynamics. The R-T instability grows to the nonlinear bubble-and-spike phase that results in the formation of high density and temperature islands near the bubbles. The calculations show that the X-ray emission is highly inhomogeneous giving rise to hot spots of dimension ~0.1 $\mu$m, in agreement with the measurements.

Douglas *et al*. (1997) used the MACH2 (Peterkin *et al*., 1993, 1998) 2-D RMHD simulation code to show that a uniform-fill gas-puff *z* pinch with a concave current sheath ("hourglass effect") reduces the growth of the MRT instability. The point is that a curved sheath introduces an axial flow along the outer edge of the load and convects the perturbations to the edges of the pinch, thereby reducing the growth rate of the MRT instability. The reduction in MRT growth could the result of velocity shear or material advection along the interface toward the electrodes.

Douglas *et al*. (1998) used the MACH2 to perform a series of 2-D RMHD calculations to investigate single and multimode growth and mode coupling for MRT instabilities in *z* pinches. Wavelengths ranging from 5.0 mm down to 1.25 mm were considered. Such wavelengths are comparable to those observed at stagnation using a random density "seeding" method. The calculations show that wavelengths resolved by less than 10 cells exhibit an artificial decrease in initial Fourier spectrum amplitudes and a reduction in the corresponding amplitude growth. Single mode evolution exhibits linear exponential growth and the development of higher harmonics as the mode transitions into the nonlinear phase. The mode growth continues to grow exponentially but at a slower rate than determined by linear theory.

Douglas *et al*. (2000*a*, 2000*b*) used the MACH2 code to perform a series of 2-D RMHD calculations to investigate the effect of long pulses (>100 ns) on the performance of both Saturn and Z drivers. Douglas *et al*. (2000*b*) present both experimental and two-dimensional computational modeling of the first long-implosion-time Z experiments. The experimental data shows broader pulses, lower powers, and larger pinch diameters compared to the corresponding short pulse data. The simulations show that the effective width of

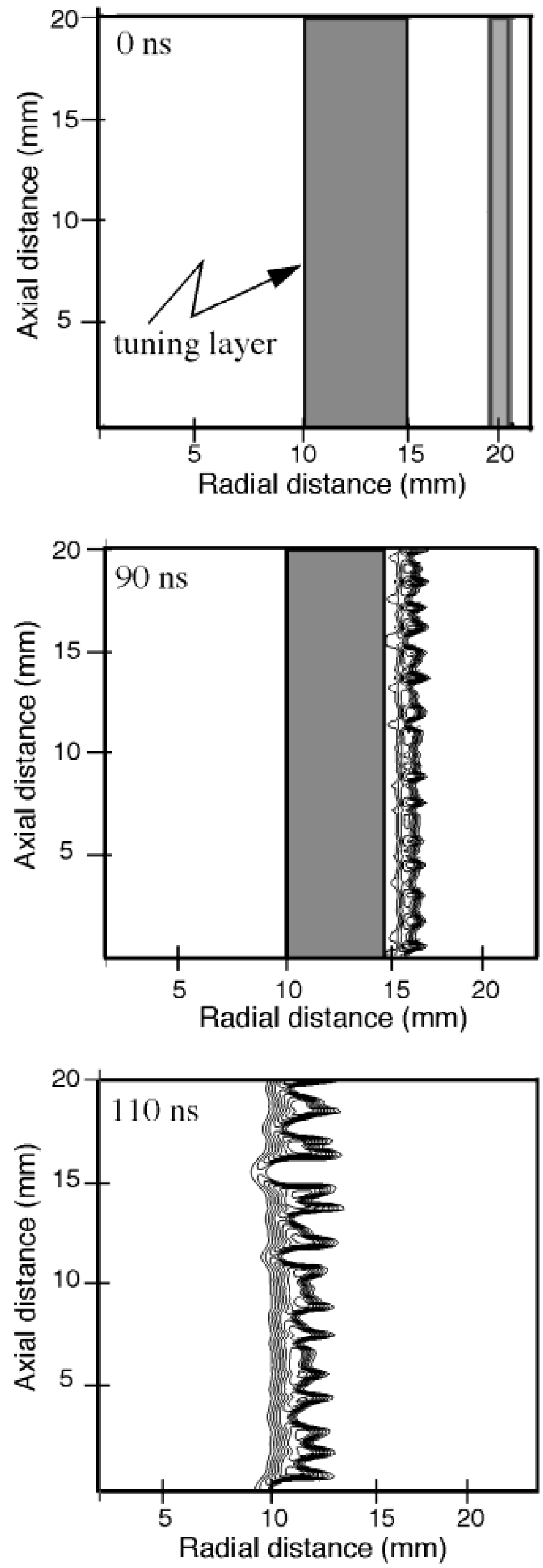


**Fig. 11.** Simulations show that the introduction of another shell downstream of a 1-mm-thick, 40-mm-diameter annular load leads to improvements in pinch quality. A 5-mm-thick inner shell is placed at 20 mm diameter. Isodensity contour plots are shown at 0 ns, 90 ns, and 110 ns into the implosion. (From Douglas *et al*., 2001.)

https://doi.org/10.1017/S0263034601194012 Published online by Cambridge University Press

the shell varies as (initial perturbation level)$^{1/2}$. Figure 10 (Douglas *et al.*, 2000*b*) shows the simulated evolution of long-pulse Saturn shot 2496 for a 1% and 5% cell-to-cell random density initial seed. By employing a nested array configuration, the pinch diameter was reduced by 50% with a corresponding increase in power of 30%. Numerical simulations suggest that load velocity is the dominating mechanism behind these results.

Douglas *et al.* (2001) used the MACH2 code to investigate the effect that load thickness plays on the mitigation of the MRT instability in fast annular *z*-pinch implosions. In particular, the effects of load thickness on the mitigation of the MRT instability and energy coupling between the plasma load and generator are addressed. Computer simulations using parameters representative of the Z driver show that increased load thickness results in lower amplitude and slightly longer wavelength MRT modes. In addition, there appears to be an optimum in implosion velocity which is directly associated with the thickness of the sheath and subsequent MRT growth. Thin, annular loads, with a thickness on the order of 1 mm that should couple efficiently to the accelerator, show a large reduction in implosion velocity due to extreme MRT development and increased load inductance. As a consequence, thicker loads on the order of 5 mm couple almost as efficiently to the generator because the MRT growth is reduced. This suggests that *z*-pinch loads can be tailored for different applications, depending on the need for uniformity or high powers. Figure 11 shows the introduction of a tuning shell downstream of a 1-mm-thick, 40-mm-diameter annular load leads to improvements in pinch quality. The density of the tuning layer is determined by equating the force due to the accrued mass to the $\mathbf{J} \times \mathbf{B}$. For this case, a 5-mm-thick tuning shell is placed at a diameter of 20 mm. Isodensity contour plots are shown at 0 ns, 90 ns, and 110 ns into the implosion.

## 7. THE FUTURE: SUPER-HIGH-POWER X-RAY SOURCES AND FUSION POWER

The most important application of *z* pinches at present is their use as X-ray and neutron sources. The relative simplicity of design, high power density, and X-ray radiation energy output in a broad spectral range make *z*-pinch sources unique for many applications, including X-ray lithography, spectroscopy and microscopy, and so forth. (Burkhalter *et al.*, 1977, 1979; Bailey, 1982; Bruno *et al.*, 1983; Spielman, 1985*b*; Pereira & Davis, 1988; Lebert *et al.*, 1989). The efficiency of transformation of the kinetic energy and/or of the thermal energy of the pinch plasma into X-ray radiation can be larger than 100% (Spielman, 1985*a*, 1985*b*)!

### 7.1. Superpower X-ray sources

High-density wire-array *z* pinches are the most powerful laboratory source of X rays. The measured optimal total X-ray energy output from several generations of fast pulse power drivers is shown in Figure 12. A remarkable result is that the optimal X-ray yield is approximately linear with the square of the current, $I^2$ (Matzen, 1997) over many orders of driver power. This result gives confidence that future super-power drivers such as X-1 at 60 MA will radiate about 15 MJ of X rays.

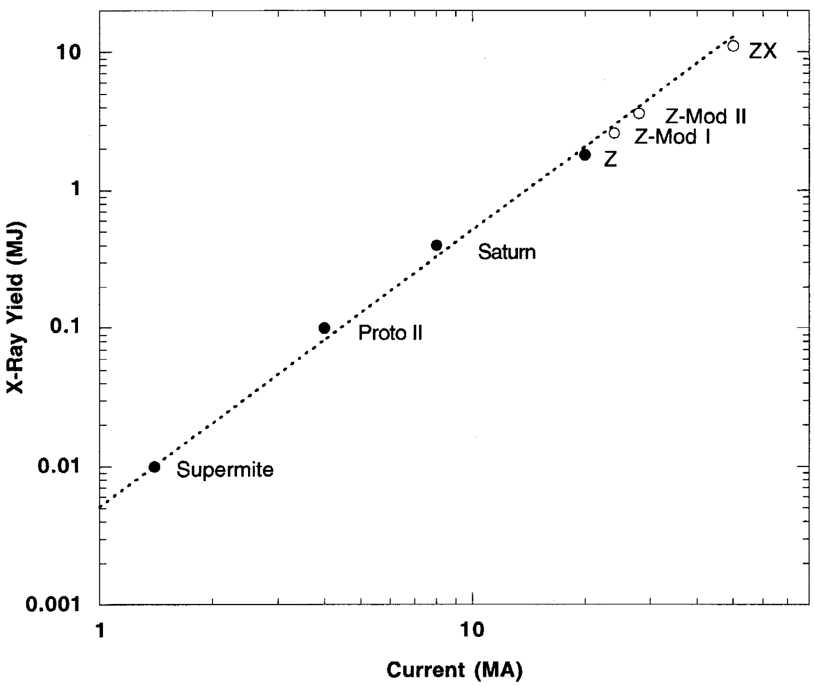


**Fig. 12.** The optimized total X-ray output from several generations of pulsed-power drivers at Sandia National Laboratories. The filled circles are measurements and the open circles are planned accelerators. The dashed line indicates that the radiated X-ray energy scales approximately as the driver power, $I^2$ (Matzen, 1997).

https://doi.org/10.1017/S0263034601194012 Published online by Cambridge University Press

### 7.2. IFE fusion power

X-ray yields of 1–2 MJ at power levels of ∼280 TW have been measured (Deeney *et al*., 1998). This breakthrough in *z*-pinch performance led to the idea of using the X rays to drive a fusion capsule. High-gain indirectly driven capsule designs that could be driven by a dual 60-MA class driver have been presented.

Very high fusion energy gains (fusion yield/X-ray yield ≈ 75) were obtained (Hammer *et al*., 1999; Olson *et al*., 1999) with 16 MJ of X rays that could be produced by a dual, 60-MA pulsed-power driver. Recently (Slutz *et al*., 2000), designs for a *z*-pinch driven IFE power plant have been advanced. These designs exploit the low cost of modern pulsed-power generators (\$10–\$20/$J_e$) and the possibility of generating fusion yields in the >1 GJ range. At these yields, the recyclable portion of the transmission line that must be replaced each shot can be fabricated at low enough cost. In addition, direct conversion schemes (Logan, 1992, 1993) can be used to produce competitive power plants (De Groot *et al*., 2000).

## 8. CONCLUSION

After 50 years, *z* pinches remain a dynamic field of research. The continuing evolution of pulse-power technology dovetails nicely with the needs of the *z*-pinch research community. The recent advances in the understanding and modeling of *z* pinches and in pulse-power technology opens a vast area of future applications and research. Indeed, why should *z* pinches not reach power levels greater than a petawatt with new drivers? The continuing development of new ways to harness the capabilities of *z* pinches in the area of thermonuclear fusion will provide tremendous excitement over the next several decades.

## REFERENCES


Alper B. (1990). *Phys. Fluids* B **2**, 1338.

Alvazov, I.K. *et al.* (1988). *Fiz. Plasmy* **14**, 197 [translation in *Sov. J. Plasma Phys.*, 1988, **14**, 110].

Alvazov, I.K. *et al.* (1990). *Fiz. Plasmy* **16**, 645 [translation in *Sov. J. Plasma Phys.*, 1990, **16**, 373].

Anderson, O.A. *et al.* (1958). *Phys. Rev.* **110**, 1375.

Artsimovich, L.A. (1958). In *Proc. Second U. N. Conf. on Peaceful Uses of At. Energy* **31**, 6.

Artsimovich, L.A. *et al.* (1964). *Sov. J. At. Energy* **17**, 886.

Bailey, J.E. *et al.* (1982). *Appl. Phys. Lett.* **40**, 33.

Baker, W.L. *et al.* (1978). *J. Appl. Phys.* **49**, 4694.

Baksht, R.B. *et al.* (1981). In *Tenth European Conf. on Controlled Fusion and Plasma Phys.*, Moscow USSR, Petit-Lancy, Switzerland: European Physics Society. p. FP-5/615.

Baksht, R.B. *et al.* (1989). *Zh. Tekh. Fiz.* **59**, 57 [translation in *Sov. Phys.-Tech Phys.*, 1989, **34**, 163.]

Baksht, R.B *et al.* (1993). *Lasers Part. Beams* **11**, 587.

Baksht, R.B. *et al.* (1994). *Third Int. Conf. Dense Z-Pinches* (Haines, M. and Knight, A., Eds.). AIP Conference Proceedings, vol. 299, p. 395. New York: AIP.

Baksht, R.B. *et al.* (1995). *Fizika Plazmy* **21**, 959 [translation in *Plasma Phys. Rep.*, 1995, **21**, 907].

Bekhtev, M.V. *et al.* (1989). *Zh. Exp. Teor. Fiz* **95**, 1653 [translation in *Sov. Phys.-JETP*, 1989, **68**, 955].

Bernstein, I.B. *et al.* (1958). *Proc. Roy. Soc. London A* **244**, 17.

Book, D.L. (1996). *Phys. Plasmas* **3**, 354.

Braginskii, S.I. (1957). *Zh. Eksp. Teor. Fiz.* **33**, 645 [*Sov. Phys. JETP*, 1958, **6**, 494].

Bruno, C. *et al.* (1983). In *Proc. of the Fifth Int. Conf. on High-Power Part. Beams, San Francisco*, CA. USA, p. 280.

Burkhalter, P.G. *et al.* (1977). *Phys. Rev. A* **15**, 700.

Burkhalter, P.G. *et al.* (1979). *J. Appl. Phys.* **50**, 705.

Burkhardt, L.C. & Lovberg, R.H. (1958). In *Proc. of the U.N. Conf. on Peaceful Uses of Atomic Energy*, Geneva: United Nations, **32**, 29.

Burns, E.J.T. *et al.* (1977). *Appl. Phys. Lett.* **31**, 477.

Campbell, E.M. *et al.* (1986). *Rev. Sci. Instrum.* **57**, 2101.

Chace, W.G. & Moore, H.K., Eds. (1959–1968). *Exploding Wires 1959–1968, Proc. of Conf. on the Exploding Wire Phenomenon*. New York: Plenum Press.

Chandrasekar, S. (1961). *Hydrodynamic and Hydromagnetic Stability*, Oxford: Clarendon.

Clauser, M.J. *et al.* (1978). *Bull. Am. Phys. Soc.* **23**, 822.

Coppi, B. (1964*a*). *Phys. Lett.* **11**, 226.

Coppi, B. (1964*b*). *Phys. Lett.* **12**, 213.

Coppi, B. (1965). *Phys. Lett.* **14**, 172.

Coppi, B. *et al.* (1966). *Nucl. Fusion* **6**, 101.

Cousins, A.W. & Ware, A.A. (1951). *Proc. Phys. Soc.* **B64**, 1959.

Deeney, C. *et al* (1989). *Second Int. Conf. Dense Z-Pinches*, (Pereira, N.R., Davis, J., and Rostoker, N., Eds.). AIP Conference Proceedings, vol. 195, p. 55. New York: AIP.

Deeney, C. *et al.* (1991). *Phys. Rev. A* **44**, 6762.

Deeney, C. *et al.* (1994). *J. Appl. Phys.* **75**, 2781.

Deeney, C. *et al.* (1997). *Phys. Rev. E* **56**, 5945.

Deeney, C. *et al.* (1998). *Phys. Rev. Lett.* **81**, 4883.

Deeney, C. *et al.* (1999). *Phys. Plasmas* **6**, 3576.

De Groot, J.S. *et al.* (1997*a*). *Phys. Plasmas* **4**, 737.

DeGroot, J.S. (1997*b*). *Fourth Int. Conf. Dense Z-Pinches*, (Pereira, N.R., Davis, J., and Pulsifer, P.E., Eds.). AIP Conference Proceedings, vol. 409, p. 157. New York: AIP.

De Groot, J.S. *et al.* (2000). Plasma Res. Group Report PRG-M-196, University of California, Davis.

Douglas, M.R. *et al.* (1997). *Phys. Rev. Lett.* **78**, 4577.

Douglas, M.R. *et al.* (1998). *Phys. Plasmas* **5**, 4783.

Douglas, M.R. *et al.* (2000*a*). *Phys. Plasmas* **7**, 1935.

Douglas, M.R. *et al.* (2000*b*). *Phys. Plasmas* **7**, 2945.

Douglas, M.R. *et al.* (2001). *Phys. Plasmas* **8**, 238.

Dukart, R.J. *et al.* (1987). In *Megagauss Technology and Pulsed Power Applications*, Fowler, C.M., Caird, R.S. and Erickson, D.J., Eds.) p. 183. New York: Plenum Press.

Felber, F.S. & Rostoker N. (1981). *Phys. Fluids* **24**, 1049.

Felber, F.S. *et al.* (1988*a*). *Phys. Fluids* **31**, 2053.

Felber, F.S. *et al.* (1988*b*). *J. Appl. Phys.* **69**, 3831.

Finn, B.S. (1971). *Br. J. for the History of Sci.* **5**, 289.

Freeman, J.R. *et al.* (1977). *Nucl. Fusion*, Suppl., **1**, 167.

Furth, H.P. (1963). *Phys. Fluids* **6**, 48.

Gol'berg, S.M. & Velikovich, A.L. (1994). *Dense Z-Pinches* (Haines, M. and Knight, A., Eds.). AIP Conference Proceedings, vol. 299, p. 42. New York: AIP.
Gorbunov, E.P. & Rosumova, K.A. (1963). *Sov. J. At. Energy* **15**, 1105 [in Russian].
Grad, H. (1966). *Phys. Fluids* **9**, 225.
Hain, Von K. *et al.* (1957). *Z. Naturforsch.* **A12**, 833.
Hammer, J.H. *et al.* (1996). *Phys. Plasmas* **3**, 2063.
Hammer, J.H. & Ryutov, D.D. (1999). *Phys. Plasmas* **6**, 3302.
Hammer, J.H. *et al.* (1999). *Phys. Plasmas* **6**, 2129.
Hsing, W.W. *et al.* (1990). Albuquerque, NM: Report SAND90-3175A, Sandia National Laboratories.
Katzenstein, J. (1981). *J. Appl. Phys.* **52**, 676.
Kruskal, M. & Oberman, C.R. (1958). *Phys. Fluids* **1**, 275.
Kruskal, M. & Schwarzschild, M. (1954). *Proc. Roy. Soc. London A* **223**, 348.
Lebert, R. *et al.* (1989). In *Second Int. Conf. Dense Z-Pinches* (Pereira, N.R., Davis, J. and Rostoker, N., Eds.) AIP Conference Proceedings, vol. 195, p. 515. New York: AIP.
Lee, Y.T. & More, R.M. (1984). *Phys. Fluids* **27**, 1273.
Liberman, M.A. *et al.* (1999). *Phys. of High-Density Z-Pinch Plasmas*. New York: Springer-Verlag.
Linhart, J.G. *et al.* (1962). *Nucl. Fusion* Supplement Part 2, 733.
Logan, B.G. (1992). *Fusion Technol.* **21**, 1784.
Logan, B.G. (1993). *Fusion Eng. and Design* **22**, 151.
Lokke, W.A. & Grassberger, WH. (1977). Lawrence Livermore National Laboratory Report No. UCRL-52276. Springfield, VA: National Technical Information Services.
Marrs, R.E. *et al.* (1983). *Appl. Phys. Lett.* **42**, 946.
Martin, T.H. *et al.* (1996). *J. C. Martin on Pulsed Power*. New York: Plenum Press.
Mather, J.W. & Williams, A.H. (1958). *Proc. Second U.N. Conf. on Peaceful Uses of Atomic Energy*, **32**, 26.
Matzen, M.K. *et al.* (1986). *J. de Physique* **47**, C6-135.
Matzen, M.K. (1997). *Phys. Plasmas* **4**, 1519.
Maxon, S. *et al.* (1985). *J. Appl. Phys.* **57**. 971.
Maxon, S. *et al.* (1996). *Phys. Plasmas* **3**, 1737.
McDaniel, D.H. *et al.* (1979*a*). *Bull. Am. Phys. Soc.* **23**, 822.
McDaniel, D.H. *et al.* (1979*b*). Report SAND79-0373A, Albuquerque, NM: Sandia National Laboratories.
McDaniel, D.H. *et al.* (1992). In *Proc. of the Ninth Int. Conf. on High-Power Part. Beams*, Washington, DC (Cooperstein, J., Ed.) p. 97. NRL.
More, R.M. *et al.* (1975). *Phys. Fluids* **31**, 3059.
Mosher, D. *et al.* (1973). *Appl. Phys. Lett.* **23**, 429.
Nielson, P.D. & Zimmerman, G.B. (1981). Lawrence Livermore National Laboratory Report No. UCRL-53123. Springfield, VA: National Technical Information Services.
Olson, R.E. *et al.* (1999). *Fusion Technol.* **35**, 260.
Pease, R.S. (1957). *Proc. R. Soc. London B* **70**, 11.
Pereira, N.R. & Davis, J.J. (1988). *J. Appl. Phys.* **64**, R1.
Peterkin, Jr., J.R. *et al.* (1993). *IEEE Trans. Plasma Sci.* **21**, 552.
Peterkin, Jr., J.R. *et al.* (1998). *J. Comp. Phys.* **140**, 148.
Peterson, D.L. *et al.* (1996). *Phys. Plasmas* **3**, 368.
Post, D.E. *et al.* (1977). *At. Data and Nucl. Data Tables* **20**, 397.
Prager, S.C. (1992). *Plasma Phys. Contr. Fusion* **34**, 1895.
Roderick, N.F. & Hussey, T.W. (1984). *J. Appl. Phys.* **56**, 1387.
Rosenbluth, M.N. (1956). Report LA-2030. Los Alamos, NM: Los Alamos Scientific Laboratory.
Rosenbluth, M.N. & Longmire C.L. (1957). *Ann. Phys.* **1**, 120.
Rosenbluth, M.N. *et al.* (1954). Report LA-1850. Los Alamos, NM: Los Alamos Scientific Laboratory.
Rudakov, L.I. (1978). *Fiz. Plazmy* **4**, 72 [*Sov. J. Plasma Phys.*, 1978, **4**, 45].
Sakharov, A.D. (1951). In *Plasma Phys. and the Problem of Controlled Thermonuclear Fusion Reactions* (Leontovich, M.A., Ed.) Vol. 1, p. 21. New York: Pergamon Press.
Sanford, T.W.L. *et al.* (1996). *Phys. Rev. Lett.* **77**, 5063.
Sanford, T.W.L. *et al.* (1997). *Phys. Fluids* **4**, 2188.
Shafranov, V.D. (1956). *At. Energy* **1**, 38 [*J. Nucl. Energy*, 1957, **5**, 86].
Shafranov, V.D. (1958*a*). In *Plasma Phys. and Problems of Controlled Thermonuclear Fusion Reactions*. Vol. 2, p. 130. Moscow: Izdatel'stvo AN SSSR; in Russian (translation, 1961, in ibid Vol. 2, p. 197. New York: Pergamon Press).
Shafranov, V.D. (1958*b*). In *Plasma Phys. and Problems of Controlled Thermonuclear Reactions*. Vol. 4, p. 61. Moscow: Izdatel'stvo AN SSSR; in Russian (translation, 1961, in ibid Vol. 4, p. 71. New York: Pergamon Press).
Shanny, R. & Vitkovitsky, I. (1969). Report. Washington DC: Naval Research Laboratory.
Sheehey, P. *et al.* (1992). *Phys. Fluids B* **4**, 3698.
Shiloh, J. *et al.* (1978). *Phys. Rev. Lett.* **40**, 515.
Slutz, S.A. *et al.* (2000). *Proc. of the 10th Int. ICENES on Emerg. Nuc. Sys.*, Petten, The Netherlands, September 24–28, 2000 (van Dam, H., and Kuikper, J., Eds.) p. 515. Delft: NRG.
Sorokin, S.A. & Chaikovsky, S.A. (1994). *Third Int. Conf. Dense Z-Pinches*, London (Haines, M. and Knight, A., Eds.) AIP Conference Proceedings, vol. 299, p. 83. New York: AIP.
Spielman, R.B. *et al.* (1985*a*). *Appl. Phys. Lett.* **47**, 229.
Spielman, R.B. *et al.* (1985*b*). *J. Appl. Phys.* **57**, 883.
Spielman, R.B. *et al.* (1989). *Second Int. Conf. Dense Z-Pinches*, (Pereira, N.R., Davis, J. and Rostoker, N., Eds.) AIP Conference Proceedings, vol. 195, p. 3. New York: AIP.
Spielman, R.B. *et al.* (1994). *Third Int. Conf. Dense Z-Pinches* (Haines, M. and Knight, A., Eds.) AIP Conference Proceedings, vol. 299, p. 404. New York: AIP.
Spielman, R.B. *et al.* (1995). *Bull. Am. Phys. Soc.* **40**, 1845.
Spielman, R.B. *et al.* (1997). In *Proc. of the Eleventh IEEE Pulsed Power Conf.*, Baltimore, MD. (Cooperstein, G. and Vitkoitsky, I., Eds.) p. 709. New York: IEEE.
Spielman, R.B. *et al.* (1998). *Phys. Plasmas* **5**, 2105.
Stallings, C. *et al.* (1979). *Appl. Phys. Lett.* **35**, 524.
Stinnett, R.W. *et al.* (1979). Report SAND79-0762A, Albuquerque, NM: Sandia National Laboratories.
Suydam, B.R. (1958). In *Proc. of the Second United Nations Conf. on Peaceful Uses of Atomic Energy*. Geneva: United Nations, **31**, 157.
Tamm, I.E. (1951). In *Plasma Phys. and the Problem of Controlled Thermonuclear Fusion Reactions* (Leontovich, M.A., Ed.) Vol. 1, pp. 1 and 35. New York: Pergamon Press.
Tayler, R.J. (1957). *Proc. R. Soc. London B* **70**, 1049.
Thronemann, P.C. (1958). In *Proc. of the Second U. N. Conf. on Peaceful Uses of Atomic Energy*. Geneva: United Nations, **32**, 3.
Thronemann, P.C. & Gowhig W.T. (1951). *Proc. Phys. Soc. B* **64**, 345.
Trubnikov, B.A. (1958). In *Plasma Phys. and Problems of Controlled Thermonuclear Reactions*. Moscow: Izdatel'stvo AN SSSR; in Russian, Vol. 1, p. 289.
Tuck, J.L. (1958). In *Proc. of the Second U.N. Conf. on Peaceful Uses of Atomic Energy*. Geneva: United Nations, **32**, 3.

Turchi, P.J. & Baker W.L. (1973). *J. Appl. Phys.* **44**, 4936.
Turner, G.L.E. & Levere T.H. (1973). In *Martinus Van Marum Life and Work*, Vol. 4 (Lefebvre, E. and De Bruijn, J.G., Eds.). Leyden: Noordhoff International Publishing.
Tuszewski, M. (1988). *Nucl. Fusion* **28**, 2033.
Velikovich, A.L. & Gol'berg, S.M. (1993). *Phys. Fluids B* **5**, 1164.
Velikovich, A.L. *et al.* (1996). *Phys. Rev. Lett.* **77**, 853.
Velikovich, A.L. *et al.* (1997). *Dense Z-Pinches*, (Pereira, N.R., Davis, J. and Pulsifer, P., Eds.) AIP Conference Proceedings, vol. 409, p. 549. New York: AIP.
Vikharev, V.D. *et al.* (1991). *Zh. Eksp. Teor. Fiz.* **99**, 1133 [translation in *Soviet Physics–JETP*, 1991, **72**, 631].
Wessel, F.J. *et al.* (1986). *Appl. Phys. Lett.* **48**, 1119.
Whitney, K.J. *et al.* (1994). *Phys. Rev E* **50**, 2166.
Zimmerman, G.B. *et al.* (1973). Lawrence Livermore National Laboratory Report No. UCRL-74811. Springfield, VA: National Technical Information Services.